Size Effects and the Problem with Percolation in Nanostructured Transparent Conductors

Sukanta De, Paul J. King, Philip E. Lyons, Umar Khan, and Jonathan N. Coleman*

School of Physics and CRANN, Trinity College Dublin, Dublin 2, Ireland

ABSTRACT Much research is underway at present to develop nanostructured transparent conductors for use as electrodes. Transparent electrodes typically require high visible transmittances, $T > 90\%$, and so must be very thin. We show that for most nanostructured films thin enough to display $T > 90\%$, the conduction can be described by percolation theory. This means DC conductivities are lower than in bulk, giving correspondingly higher sheet resistances, R_s. To improve our understanding of the consequences of this, we develop a model which relates T to R_s in the percolation regime. We define a percolative figure of merit, Π, for which high values result in high T and low R_s. High values of Π are achieved for high DC conductivity and low optical conductivity. In addition, the film thickness, t_{min}, where the DC conductivity first deviates from its bulk value and the percolation exponent, n, must both be as low as possible. We find that this model fits extremely well to much of the data in the literature. We demonstrate that t_{min} scales linearly with the smallest dimension of the nanostructure in question (*i.e.*, diameter for wires or thickness for flakes). This clearly confirms that low diameter nanowires or thin platelets are best for transparent conducting applications. We predict the properties of silver nanowire networks to improve as wire diameter is decreased. Networks of wires with $D < 20$ nm should display properties superior to the best ITO. We demonstrate the deficiencies of standard bulk theory and the importance of understanding percolation by measuring R_s and T for networks of silver flakes. We measure the bulk ratio of DC to optical conductivity to be ~35, suggesting $R_s = 100$ $\Omega/\square$ and $T = 90\%$ are attainable. However, the large flake thickness results in high t_{min} and so low Π, resulting in actual values of $T = 26\%$ for $R_s = 100$ $\Omega/\square$. This makes this material completely unsuitable for transparent conductor applications.

KEYWORDS: transparent conductor · percolation · figure of merit · nanowire · nanotube

Transparent conductors play an important role in modern electronics. Commercially, this area is dominated by doped metal oxides, most commonly indium tin oxide (ITO). However, the rising cost of indium has sparked a search for a replacement material in recent years. While alternative metal oxides such as fluorine tin oxide display good performance, all such materials are inherently brittle.[1,2] This makes them unsuitable for the expected new wave of flexible displays. Thus, over the past decade, many groups have been searching for flexible, low-cost transparent conductors, which can be deposited at low temperature to facilitate plastic-based electronics. Such materials will have to compete with ITO on performance, achieving sheet resistance of $R_s < 100$ $\Omega/\square$, coupled with transmittance $T > 90\%$.[3] Some of the most exciting potential ITO replacements have been nanostructured materials such as networks of carbon nanotubes[4−17] or metal nanowires[18−21] and disordered films of exfoliated graphene flakes.[3,22−25] Such materials have displayed superlative performance with silver nanowire networks displaying sheet resistances of ~15 $\Omega/\square$ coupled with transmittances of $\sim85\%$.[18]

In transparent conductor research, it is critical to rate the performance of new materials and benchmark them against known standards. This is generally achieved using figures of merit (FoMs). In the past, FoMs have generally been based on the Lambert−Beer law:

$$T = e^{-\alpha t} \tag{1}$$

where α is the absorption coefficient and t is the film thickness. By combining this expression with the definition of sheet resistance (for a bulk-like film)

$$R_s = (\sigma_{DC,B} t)^{-1} \tag{2}$$

where $\sigma_{DC,B}$ is the bulk DC conductivity of the film, to eliminate t, one obtains a relationship between T and R_s:

$$T = e^{-\alpha/\sigma_{DC,B} R_s} \tag{3}$$

Here, the value of R_s for a given T is controlled by $\sigma_{DC,B}/\alpha$, with high values of this quantity giving high T coupled with low R_s. Thus, $\sigma_{DC,B}/\alpha$ can be considered a figure of merit. A number of authors have proposed FoMs based on similar analysis.[26−31]

In the specific area of transparent conductors from nanostructured materials, a slightly

different but analogous system is often used. Here, the transmittance is expressed using[32]

$$T = \left(1 + \frac{Z_0}{2}\sigma_{Op}t\right)^{-2} \quad (4)$$

where Z_0 is the impedance of free space (377 Ω) and σ_{Op} is the optical conductivity (expanding eqs 1 and 4 shows that $\sigma_{Op} \approx \alpha/Z_0$ to first order). We note that, like eq 1, this expression is independent of the connectivity of the nanostructures forming the film and so applies even to very thin films.[6,18,24] As before, eq 4 can be converted to an expression relating T and R_s:

$$T = \left(1 + \frac{Z_0}{2R_s}\frac{\sigma_{Op}}{\sigma_{DC,B}}\right)^{-2} \quad (5)$$

Here the FoM is the ratio of the DC to optical conductivity, $\sigma_{DC,B}/\sigma_{Op}$. The authors favor the latter expression simply because of the aesthetic advantages of a dimensionless FoM. However, we note that eqs 3 and 5 are essentially equivalent (i.e., by expanding to first order).[4] In addition, in both eqs 3 and 5, we use the bulk value of the DC conductivity as is implicitly assumed in all transparent conductor papers. However, as we will see below, this is not always appropriate. Using eq 5, the requirement that $R_s < 100\,\Omega/\square$ coupled with transmittance $T > 90\%$ can be stated very simply as $\sigma_{DC,B}/\sigma_{Op} > 35$. This has been surpassed for networks of silver nanowires with values of $\sigma_{DC,B}/\sigma_{Op} > 400$ reported.[18]

RESULTS AND DISCUSSION

Deviation from Bulk-like Behavior for Thin Films. This would suggest that the problem of ITO replacement has been solved. Unfortunately, things are not so simple. If one inspects data for T versus R_s for silver nanowire networks,[18] one finds that eq 5 only applies to the data at relatively low R_s, corresponding to thick films (Figure 1, black dashed line). For $R_s > 3\,\Omega/\square$, the data deviate significantly from the theoretical line. While eq 5 would lead one to expect $R_s = 7\,\Omega/\square$ for $T = 90\%$, in reality, $R_s \sim 100\,\Omega/\square$ for $T = 90\%$ was observed, a significantly less impressive result. In fact, the same behavior is ob-
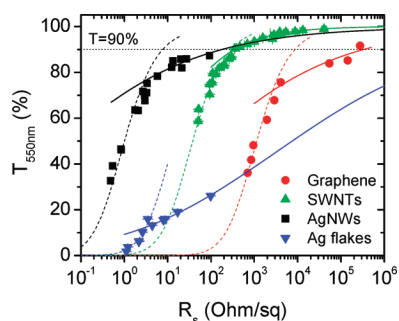

Figure 1. Transmittance (550 nm) plotted as a function of sheet resistance for thin films prepared from four nanostructured materials, graphene, single-walled carbon nanotubes, silver nanowires, and silver flakes. The dashed lines represent fits to the bulk regime using eq 5, while the solid lines represent fits to the percolative regime using eq 11.

served for other nanostructured materials. In Figure 1, we have included data for single-walled nanotubes[6,33] and graphene[24] published by our group. The same behavior can be observed in published data for a large number of nanostructured materials (see below). In most cases, the deviation from the expected behavior (dashed lines) begins to occur for films with $T < 90\%$. This is important as it means the expected bulk-like behavior does not occur in the technologically relevant regime ($T > 90\%$).

In fact, the reason for such behavior is straightforward. Below some critical thickness, t_{min}, films of nanostructured materials stop behaving like bulk and the DC conductivity begins to decrease with decreasing thickness. This behavior has been described for networks of nanotubes,[6,7] nanowires,[18] and graphene sheets[24] and is reminiscent of electrical percolation. Percolation is the onset of conductivity across a previously insulating region once conducting links have been added at a density exceeding some critical value, the percolation threshold. As more links are added, new conducting paths are formed and the conductivity increases. For example, when conducting rods are randomly deposited in-plane, the conductivity follows the percolation scaling law, $\sigma_{DC} \propto (N_A - N_{A,c})^\alpha$, where N_A is the number of rods per unit area, $N_{A,c}$ is percolation threshold, and α is the critical exponent. We note that this expression is only valid close to the percolation threshold.[34]

However, as more rods are added, eventually the network is extensive enough that all rods are interconnected in a continuous network. In principle, such a situation should be far enough from the percolation threshold such that the percolation scaling law no longer applies. However, this does not mean that the conductivity stops increasing as new rods are added. Studies on nanotube networks show that the conductivity continues to increase long after a dense continuous network is formed.[6] In fact, while the percolation threshold has been shown to occur for nanotube networks of average thickness of ~1 nm,[33] the conductivity keeps increasing with thickness until the networks are ~40 nm thick when the behavior becomes bulk-like.[6,33] (N.B. The thicknesses quoted above are effective thicknesses (see Figure 3B) and represent the thickness of a film with a given N_A and uniform density, ρ_N: $t = N_A\langle V_{cond}\rangle\rho_{cond}/\rho_N$, where $\langle V_{cond}\rangle$ is the average volume of the conducting links and ρ_{cond} is their density. For thin films, ρ_N is taken to be the same as that of a very thick network. We note that this definition of t allows the existence of films with thickness below that of the conducting entities making up the film.)

The behavior at thicknesses greater than a few nanometers is distinct from true percolation and probably occurs as non-uniformities associated with thin networks get smoothed out as the thickness increases (see below).[6,18,24] We can think of this as an intermediate regime between true percolative behavior and bulk be-
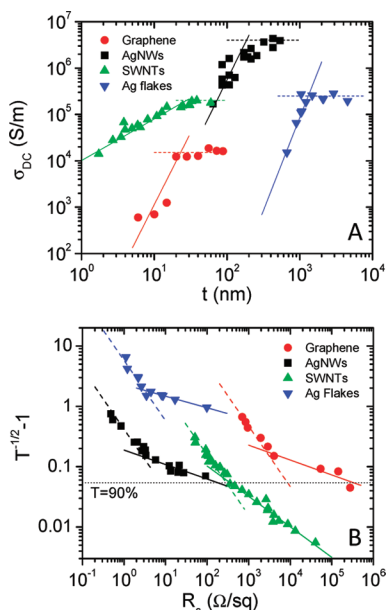
Figure 2. (A) DC conductivity plotted as a function of estimated film thickness for the materials shown in Figure 1. The dashed lines represent the bulk conductivity, while the solid lines represent fits to the percolative regime using eq 7. **(B)** Same data as plotted in Figure 1 are represented as $T^{-1/2} - 1$ vs R_s on a log−log plot. Note $T^{-1/2} - 1$ is proportional to film thickness. The dashed lines represent fits to the bulk regime using eq 5, while the solid lines represent fits to the percolative regime using eq 11.

havior. However, we note that percolation-like conductivity scaling has been observed for a number of systems far from the percolation threshold.[35−37] In fact, for the work described in ref 33, the conductivity data were consistent with a single power law extending from $t = 1$ nm all the way to $t = 40$ nm, where the transition to bulk behavior occurred. This suggests that the conductivity of nanostructured transparent conducting networks in the intermediate regime can be described by a percolation-type power law with exponent similar to that in the true percolation regime. We illustrate this by plotting the measured conductivity, σ_{DC}, for the materials plotted in Figure 1 as a function of estimated film thickness (as reported in the relevant publications, Figure 2A). In each case, below some well-defined thickness, the conductivity becomes thickness-dependent, displaying approximate power law behavior, suggestive of percolation. However, in all cases, these films are so thick that this is likely to reflect the intermediate regime rather than the true percolative regime. As such, for the rest of this paper, we will assume that a percolation-like scaling law can be extended into the intermediate regime. For simplicity, we will refer to thickness-dependent conductivity as percolation, although (as discussed above) this is not true in the strictest sense.

Looking at the data for SWNTs in Figure 1, one might argue that percolation is not a serious problem as it only becomes an issue for films that are extremely thin and so not industrially relevant. However, this is not gener-

ally the case, as can be seen for the data for graphene and the AgNWs. In fact, one can imagine a scenario where the bulk value of $\sigma_{DC,B}/\sigma_{Op}$ meets industry standards (i.e., 35 or greater) but where percolation is first observed for films so thick as to render the material completely unviable in practical terms. To illustrate this, we prepared films from silver nanoflakes (flake thickness, $D \approx 360$ nm) and measured R_s, T, and t for a range of film thicknesses (see Methods and Supporting Information). These data are included in Figures 1 and 2. These nanoflakes have a bulk FoM of $\sigma_{DC,B}/\sigma_{Op} = 35$, suggesting they are a promising candidate for ITO replacement. However, percolation is first observed at $t_{min} \approx 1300$ nm; for thicknesses below this, T increases very slowly with increasing R_s. As a result, these materials are unsuitable for use as transparent electrodes. This illustrates that bulk figures or merit such as $\sigma_{DC,B}/\sigma_{Op}$ or $\sigma_{DC,B}/\alpha$ cannot predict performance for many nanostructured materials.

Relationship between T and R_s in the Percolation Regime. Because of this phenomenon, we believe it critical to fully understand the relationship between T and R_s in the percolation regime. To do this, we will derive an expression, analogous to eq 5 but relevant in the percolation regime. The percolation scaling law discussed above can be expressed in terms of film thickness rather than conductor number density (see expression given above):[8]

$$\sigma_{DC} \propto (t - t_c)^n \qquad (6)$$

Here t_c is the threshold thickness and n is the percolation exponent. As discussed above, we assume that this expression holds in the thickness regime under study. However, we use the exponent n rather than α to illustrate that the exponent in the thicker intermediate regime is not necessarily identical to the true percolation exponent.[37] Scaling as described by eq 6 has been observed for thin films of carbon nanotubes by a number of researchers.[8,17,38] For a network with conductivity high enough to be industrially relevant, $t \gg t_c$, allowing us to write

$$\sigma_{DC} = \sigma_{DC,B}(t/t_{min})^n \qquad (7)$$

Here, as described above, the conductivity reaches its bulk value, $\sigma_{DC,B}$, at thickness t_{min}. The measured sheet resistance, R_s, is related to the actual DC conductivity by $R_s = (\sigma_{DC}t)^{-1}$. Note that this expression differs from eq 2 because we now realize that σ_{DC} can differ from its bulk value ($\sigma_{DC,B}$) for thin films. Substituting eq 7 into the expression for R_s given above, we get the sheet resistance of a percolation network:

$$R_s = (\sigma_{DC,B}(t/t_{min})^n t)^{-1} = (\sigma_{DC,B}t^{n+1}/t_{min}^n)^{-1} =$$

$$\frac{t_{min}^{n+1}}{t_{min}\sigma_{DC,B}t^{n+1}} \qquad (8)$$

Solving for t and substituting into eq 4, we obtain:

$$T = \left(1 + \frac{Z_0}{2}\sigma_{\text{Op}}t_{\min}(t_{\min}\sigma_{\text{DC,B}}R_s)^{-1/n+1}\right)^{-2} \quad (9)$$

This can be rewritten as

$$T = \left[1 + \frac{1}{2}\left(\frac{Z_0}{R_s}\right)^{1/(n+1)}\left(\frac{(Z_0 t_{\min}\sigma_{\text{Op}})^n}{\sigma_{\text{DC,B}}/\sigma_{\text{Op}}}\right)^{1/(n+1)}\right]^{-2} \quad (10)$$

We note that this expression reverts to eq 5 when $n = 0$ as expected. We can express eq 10 more compactly as

$$T = \left[1 + \frac{1}{\Pi}\left(\frac{Z_0}{R_s}\right)^{1/(n+1)}\right]^{-2} \quad (11)$$

where we denote Π as the percolative FoM:

$$\Pi = 2\left[\frac{\sigma_{\text{DC,B}}/\sigma_{\text{Op}}}{(Z_0 t_{\min}\sigma_{\text{Op}})^n}\right]^{1/(n+1)} \quad (12)$$

Π is a dimensionless number where large values of Π give low R_s coupled with high T. Equation 11 suggests that the percolative regime can be identified as a straight line on a log−log plot of $T^{-1/2} - 1$ *versus* R_s (equivalent to a graph of t *vs* R_s). Fitting these data then gives both n and Π. We plot the data for all four materials shown in Figure 1 in this form in Figure 2B. For each curve, it is clear that two regimes are present; a range with a slope of -1, consistent with eq 5 (the bulk regime) and a region with less negative slope, described by eq 11. By fitting both regimes, we obtain $\sigma_{\text{DC,B}}/\sigma_{\text{Op}}$, Π, and n for each material which we report in Table 1. We have also reproduced the fit, plotted as $T(R_s)$, to describe the percolative region in Figure 1. In all cases, very good agreement is found. We note that the exponents n vary from 1 to 4. This range is within the bounds expected for true percolation exponents (see below), suggesting that n and α may indeed be similar. We note that the percolation exponents are generally found by plotting σ_{DC} *versus* t as in Figure 2A. However, because of the inherent difficulty of measuring t in thin nanostructured films, the data are generally scattered. This shows that finding n by fitting R_s and T data using eq 11 is probably superior. We also note that the bulk and percolative FoMs follow a similar order (AgNWs > AgFlakes > SWNTs > graphene, for bulk FoM). The difference is that, when ranked by Π,
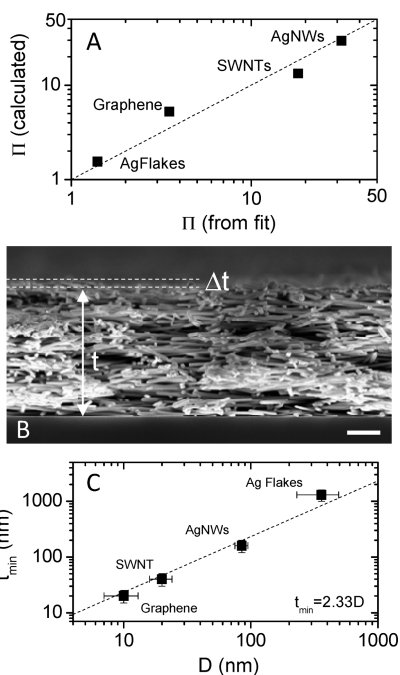

Figure 3. (A) Percolative figure of merit, Π, calculated using eq 12 plotted as a function of the value of Π found by fitting the data in Figure 2B with eq 11. (B) SEM image of the cross section of a thick network of AgNWs (scale bar = 1 μm). The dashed lines illustrate the non-uniformity in film thickness, Δt. (C) Film thickness where percolation begins, $t_{\min}$, plotted as a function of the smallest dimension of the nanostructured material making up the film, D. For example, for nanotubes or nanowires, D is the diameter, while for platelets, D is the thickness.

the silver flakes come last in keeping with their poorer thin film performance.

All of the parameters in eq 12 are now known, $\sigma_{\text{DC,B}}/\sigma_{\text{Op}}$, Π, and n from the fits described above while σ_{Op} can be found from the thickness dependence of the film transmittance using eq 4 (see refs 6, 18, 24, and 33 and the Supporting Information; values reported in Table 1).[5,6,18] This allows us to calculate Π from eq 12 and to test the consistency of the calculated value of Π with that found from fitting the data in Figure 2B. We plot the calculated values as a function of the fitted values in Figure 3A. We find almost perfect agreement. We note that the different parameters in eq 12 are found from different portions of the data; Π and n from the percolative regime, $\sigma_{\text{DC,B}}/\sigma_{\text{Op}}$ from the bulk regime, and $t_{\min}$ from the point of their intersection. The agreement shown in Figure 3A confirms that these regimes are correlated as predicted by eq 12.

TABLE 1. Values of $\sigma_{\text{DC,B}}/\sigma_{\text{Op}}$, Π, and n Found from Fitting the Curves in Figure 2B[a]

	ref	$\sigma_{\text{DC,B}}/\sigma_{\text{Op}}$	Π	n	σ_{Op} (S/m)	$t_{\min}$ (nm)	D (nm)
AgNWs	18	415	31.7	1.9	6472	160	85
SWNTs	6, 33	11.2	18.2	1.0	1.6×10^4	40	20
graphene	24	0.7	3.5	3.1	3.3×10^4	20	10
Ag flakes	Supporting Information	35	1.4	4.0	6790	1300	360

[a]Values of σ_{Op} and $t_{\min}$ were found by analysis of the thickness dependence of the T and R_s data as described in the relevant papers (see text) or in the Supporting Information. D was taken directly from the relevant papers or the Supporting Information.

TABLE 2. Values of $\sigma_{DC,B}/\sigma_{Op}$, Π, and n Found from Fitting the Data from the Literature with Equations 5 and 11[a]

	$\sigma_{DC,B}/\sigma_{0p}$	Π	n	comment
carbon-based films				
Green et al.[11]	no data	3.3	0.75	unsorted SWNTs
Green et al.[11]	4.8	9.4	0.65	sorted SWNTs (M)
Green et al.[11]	3.5	8.7	0.91	sorted SWNTs (M)
Pei et al.[14]	no data	13.1	1.04	SWNTs
Chandra et al.[10]	8.5	12.3	0.50	pristine SWNTs
Chandra et al.[10]	19.5	23.8	0.36	doped SWNTs
Li et al.[12]	2.4	4.7	0.64	pristine SWNTs
Li et al.[12]	11.0	9.1	1.60	doped SWNTs
Manivannan et al.[13]	3.8	9.6	0.82	SWNTs
Unalan et al.[17]	no data	2.6	1.49	SWNTs
Parekh et al.[16]	1.2	no data	no data	SWNTs
Parekh et al.[16]	5.1	no data	no data	doped SWNTs
Dan et al.[4]	4.5	no data	no data	SWNTs
Dan et al.[4]	11.3	no data	no data	doped SWNTs
Wu et al.[22]	1.7	4.7	0.51	reduced graphene oxide
metallic films				
Rathmell et al.[20]	no data	6.2	6.50	CuNWs deposited
Wu et al.[21]	106	48	0.83	CuNWs fused
O'Connor et al.[39]	72	4.7	5.3	thin Ag film

[a]Note we have not included the well-known data of Geng et al.[7] The reason for this is the data presented in this paper appear inconsistent; the T vs R_s data fit very well to the bulk expression (eq 5) for all T. However, the σ_{DC} vs t data clearly resemble a percolating system. The reason for this discrepancy is unclear.

Applying This Model to Data from the Literature. Equation 11 should apply to the low thickness (high T) regime for all nanostructured thin films. We have attempted to verify this by fitting eq 11 to published data. To do this, we identified a number of papers which presented R_s and T for nanostructured (nanotubes, nanowires, graphene, and metal) thin films as a function of film thickness. We extracted the data and plotted $\log(T^{-1/2} - 1)$ versus $\log(R_s)$. In some cases, the data displayed only the bulk regime (slope -1). Typically, such films did not extend to very low thickness and did not generally display transparencies greater than 90%. However, in most cases (8 out of 10 for nanotubes, not counting doped samples), the data displayed two regimes: bulk and percolative. By fitting both regimes, we found $\sigma_{DC,B}/\sigma_{Op}$, Π, and n. In all cases, the fits are very good. These values are presented in Table 2. Examples of a subset of the fits of eq 11 to the data are shown in Figure 4 for (A) carbon-based films and (B) metal-based films. As expected, data for $\sigma_{DC,B}/\sigma_{Op}$ lies in the range of 1.7−20 for carbon-based films but is considerably higher for metallic films, up to 108 for CuNWs.[21] The carbonaceous films have $3 < \Pi < 24$, with higher values observed for the metallic films, up to 48 for fused copper nanowires.[21] Perhaps surprisingly, the model also fits very well to data for thin silver films.[39] This may be due to island formation during the early stages of film growth.

Interestingly, n varied widely from 0.36 to 6.5. This range is wider than that expected from the literature where networks of carbon nanotubes have displayed $1.0 < n < 2.75$.[8,17,33,38] If n is similar to the true percolation exponent, α, then values of $n < 1$ are rather sur-

prising. However, they are not impossible. While early work predicted a universal percolation exponent of $\alpha_{un} = 1.3$ in two dimensions,[34] later computer modeling showed the breakdown of universality in certain two-dimensional systems, leading to exponents which could be greater or less than α_{un}.[40] In addition, it is widely accepted that exponents can be considerably larger than the universal value in three dimensions.[41−43] On the
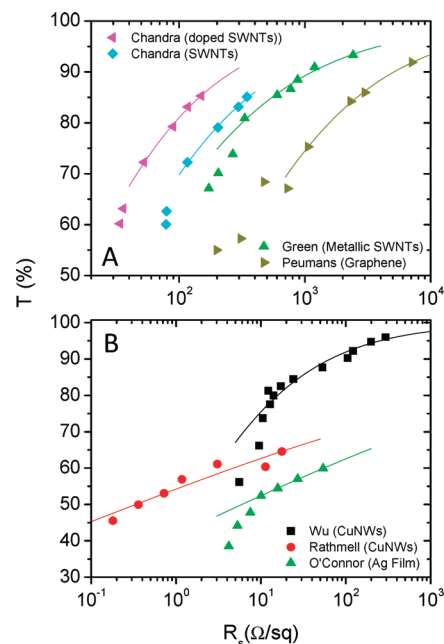

Figure 4. Transmittance plotted as a function of sheet resistance for data for the literature. (A) Carbon-based films (nanotubes or graphene, refs 10, 11, 22) and (B) metal-based films (nanowires and a thin metal film, refs 20, 21, 39). In all cases, the fits are made using eq 11 applied to the percolative regions only.

other hand, it is possible that, in some cases, $n < \alpha$, explaining the discrepancy.

Requirements of a Good Transparent Conductor. We can now consider what makes a good nanostructured transparent conductor. Ideally, bulk-like behavior would hold down to film thicknesses low enough to give $T > 90\%$. In this case, eq 5 applies and we want $\sigma_{DC,B}/\sigma_{Op}$ as high as possible. However, as shown in Figure 1, this does not generally occur. In reality, films thin enough to display $T > 90\%$ tend to fall in the percolative regime. Here eq 11 holds, and we require Π to be as large as possible (eq 12). As in the bulk case, this means we need large values of $\sigma_{DC,B}/\sigma_{Op}$. Also, intuitively, a low value of σ_{Op} is required. However, we can also identify two further requirements: t_{min} and n (as we will see below) must both be as small as possible.

Can We Control t_{min}? It is worth considering what controls t_{min}. In previous papers,[6,18] we suggested that t_{min} scales with the smallest dimension, D, of the nanostructure forming the network. This smallest dimension would be the diameter in the case of wires or nanotubes or the flake thickness in the case of graphene or silver flakes. The rationale behind this was that, once the film was a few times thicker than D, non-uniformities in the network would have averaged out and it could be considered bulk-like. We can illustrate this using Figure 3B. This is an image of the cross section of a relatively thick network of AgNWs. Such images are often used to measure film thickness as shown. However, it is clear from this image that the film thickness is slightly non-uniform as illustrated by the dashed lines. The degree of non-uniformity, Δt, is on the order of the wire diameter, D. For thick films such as that shown, this non-uniformity has no effect on the film conductivity. However, for films with thickness approaching D and below, this non-uniformity will translate into non-uniformity of the network as a whole. Effectively, N_A will vary from place to place within the network, resulting in a significant reduction in DC conductivity as the thickness is decreased. Such thickness-dependent non-uniformities have been observed for a number of nanostructured films.[5,6,18,24] Thus, we expect t_{min} to scale with D. We can illustrate this behavior with a combination of published data and data for the silver flakes measured as part of this study.

We take measurements of D from our previous work for SWNT bundles[6,33] and AgNWs[18] and graphene films.[24] (We note that, for graphene, $D = 10$ nm. This is because, during film formation, the graphene sheets aggregated into rather thick graphitic flakes.) In addition, we measured the thickness of the Ag flakes to be $D = 360 \pm 100$ nm. We take t_{min} from the relevant papers (the Supporting Information for Ag flakes). We plot t_{min} versus D in Figure 3C, finding very good linearity as described by $t_{min} = 2.33D$. This makes it absolutely clear, to reduce t_{min} and so enhance performance, it is necessary to use nanotubes/nanowires with low diameter or

nanoplatelets with low thickness. For example, extremely good results have been achieved with AgNWs with diameter of ~ 85 nm.[18] If AgNWs with significantly lower diameter could be obtained, even better results might be expected. We note that, nominally, SWNTs have $D \sim 1$ nm. However, during film formation, SWNT always aggregate into bundles with $D \gg 1$ nm. Frustrating this bundling process would greatly reduce D and so t_{min}, leading to better films. In any case, it is important to emphasize that this is a general result. Reduction of the shortest dimension (D) of a conducting nanostructure will result in higher percolative figure of merit, Π, and so improved T and R_s. Thus, low diameter nanowires or nanotube bundles are required. Alternatively, thin metal platelets could result in good quality films. While networks of graphene flakes initially seemed promising, due to their high absorbance, it is unlikely that they will reach industry standards of $T \sim 90\%$ for $R_s < 100$ $\Omega/\square$.[3]

As described above, reduction of D should result in significantly improved films. However, it is important to realize that, if D could be decreased dramatically, it would be possible to produce film such that $T = 90\%$ was achieved in the bulk rather than the percolative regime. This would result in significantly reduced R_s. By substituting $t_{min} = 2.33D$ into eq 4, we can show that this occurs when $D < 0.05/Z_0\sigma_{Op}$. For AgNWs, this gives $D < 18$ nm, much lower than what is commercially available. (We note that this estimation assumes that σ_{Op} is invariant with D. While this is unlikely, we know of no studies giving the actual dependence of σ_{Op} on D; see below for more discussion.)

Effect of n on Film Properties. Before discussing the effect of n on film properties, we note that, as described above, n may be very close to the true percolative exponent, α (i.e., $n \approx \alpha$). In that case, it is worth considering what controls α in a percolative system. The percolation exponent was originally expected to take on the universal value of $\alpha_{un} = 2$ for a three-dimensional system or $\alpha_{un} = 1.3$ for a two-dimensional system.[34] By the late 1980s, it was realized that higher values were possible.[41,42,44] Such non-universal exponents have been linked to the presence of a distribution of junction resistances at conductor−conductor junctions.[37,42,43,45] For example, in three-dimensional films, it has been shown that for a distribution of junction resistances, $\alpha > \alpha_{un}$ with $\alpha - \alpha_{un}$ controlled by the shape of the distribution.[42−44] For nanotube films, it is known that the junction resistances can be large and their distributions quite broad.[46] This is partly due to residual surfactant or other dispersants remaining trapped at internanotube junctions and so increasing both the position and width of junction resistance distribution. Post-treatment can be used to remove the surfactant thus improving $\sigma_{DC,B}/\sigma_{Op}$.[7,46] As can be seen from Table 2, such treatment also tends to change n. We propose that post-treatments might be developed
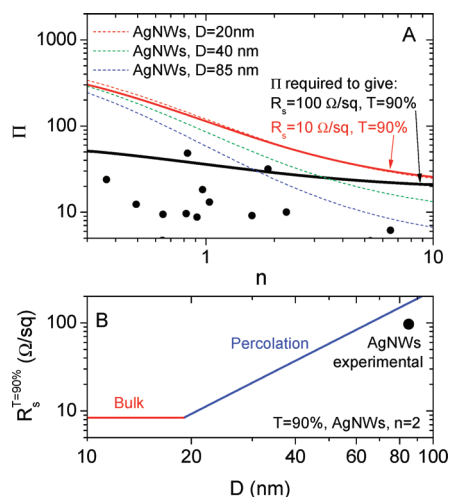
Figure 5. (A) Percolative figure of merit, Π, plotted against conductivity exponent, n. The dashed lines represent the values of Π calculated from eq 12 for three different values of t_{min}, and so D. The solid lines represent the values of Π required to give certain combinations of T and R_s, as calculated from eq 11. The circles represent the data from Tables 1 and 2. The only data above the black solid line represent silver and copper nanowires. (B) Achievable sheet resistance for films with $T = 90\%$, plotted as a function of nanowire diameter. This curve was calculated using eq 10 incorporating $t_{min} = 2.33D$ and assuming $n = 2$, using data for silver nanowires given in Table 1, that is, $\sigma_{DC,B}/\sigma_{Op} = 415$ and $\sigma_{Op} = 6472$ S/m. As described in the text, for films prepared with wires of $D < 18$ nm, $T = 90\%$ occurs in the bulk regime (*i.e.*, $t > 2.33D$). Thus, for $D < 18$ nm, no further improvements are observed. The data point shows experimental data for a AgNW film with $T = 88\%$, as reported by De *et al.*[18]

which can both improve $\sigma_{DC,B}/\sigma_{Op}$ and controllably tune n, resulting in significant increases in Π.

The optimum value of n for transparent conductors is less clear than the requirements for $\sigma_{DC,B}/\sigma_{Op}$, σ_{Op}, and t_{min}. This is because n appears not only in eq 11 but also in eq 12. As a starting point, we must consider how n effects Π. Consider a network of silver nanowires. We assume that both $\sigma_{DC,B}/\sigma_{Op}$ and σ_{Op} are fixed, while t_{min} depends on wire diameter as described above. (We make the approximation that both σ_{Op} and $\sigma_{DC,B}/\sigma_{Op}$ are invariant with wire diameter as discussed below.) The exponent n will vary from network to network as discussed above. We can use eq 12 to calculate Π as a function of n for different values of D (*i.e.*, different t_{min}), as shown in Figure 5A. We see that Π increases with decreasing n, suggesting that lower n values would be preferred (dashed lines). In addition, Π increases with decreasing wire diameter, D, simply because $t_{min} \propto D$.

However, because n also appears in eq 11, we must also consider how n effects the value of Π required to attain a given R_s and T. The minimum industry standards for transparent conductors are usually quoted as $T > 90\%$ for $R_s < 100$ $\Omega/\square$.[3,21] We can use eq 11 to plot the minimum value of Π required to give these values as a function of n, as shown in Figure 5A (we also plot the minimum value of Π required to give $T > 90\%$ for R_s

< 10 $\Omega/\square$). We find that the required value of Π tends to increase with decreasing n (solid lines). This tends to cancel out the advantage of low values of n (low n may give higher Π, but as n is decreased, ever higher Π is required). However, the dashed lines tend to increase faster than the solid lines as n is decreased. This means that, overall, it is advantageous to have a network with lower n. Ultimately, this means that reducing the spread in interconductor resistances would improve film properties. It is interesting to note that if we could produce wires with $D = 20$ nm we would achieve values of Π which match the value of Π required to give $T = 90\%$ for $R_s = 10$ $\Omega/\square$ *independent of n*. This reinforces the importance of decreasing D in these systems. In any case, if a method could be found to control n for a given system, reducing n should result in increases in T and reductions in R_s, leading to improved thin films.

Dependence of R_s on D for High T Films. We note that we have calculated $n = 1.9$ for the AgNW data of De *et al.*, close to the universal percolation exponent for three dimensions.[18] Assuming n to be invariant with wire diameter, we can calculate the sheet resistances which might be achieved for films of silver nanowires with $T = 90\%$, $R_s^{T=90\%}$, as a function of nanowire diameter using eq 10 and taking $t_{min} = 2.33D$ (Figure 5B). We use the values of the σ_{Op} and $\sigma_{DC,B}/\sigma_{Op}$ given in Table 1 assuming them to be diameter-independent (see below for justification). We see a steady decrease from $R_s^{T=90\%} \approx 100$ $\Omega/\square$ for $D \approx 60$ nm to $R_s^{T=90\%} \approx 10$ $\Omega/\square$ for $D \approx 20$ nm. As described above, for $D < 18$ nm, $T = 90\%$ films occur in the bulk regime and no further improvements from further decreases in D.

The analysis just described assumes the conductivity exponent, n, and both the DC and optical conductivities of the network to be diameter-independent. This is probably the case for n as changing the rod diameter in the intermediate regime would change only the characteristic length scale of the system (as long as the aspect ratio remained high) and so should not effect n. In the case of the network conductivity, σ_{DC} probably increases with decreasing wire diameter. The reason for this is that the diameter dependence of σ_{DC} depends on two factors: the wire conductivity and the network connectivity. The conductivity of silver nanowires is expected to decrease by a factor of 2 as D goes from 50 to 25 nm.[47,48] However, due to enhancement in connectivity, the network conductivity should increase as D decreases, potentially canceling the effect of wire conductivity.[49,50] We have calculated the overall effect of wire diameter on network conductivity in the Supporting Information. We find that, as long as the network connectivity displays diameter dependence similar to that suggested in the literature, σ_{DC} either stays constant or increases with decreasing wire diameter (N.B. higher values of σ_{DC} give better films). Unfortunately, we have found no information on the dependence of the op-

tical conductivity of a nanowire network on wire diameter. However, we note that, as long as σ_{Op} remains constant or decreases with decreasing diameter, the result will be sheet resistances similar (or even lower) than those reported in Figure 5B. In fact, this seems likely as we would expect σ_{Op} to scale with nanowire conductivity, which does indeed decrease with decreasing wire diameter.[47] This fact, coupled with the expectation that σ_{DC} actually increases with decreasing D, means that the data in Figure 5B are probably a worst case scenario. This means that sheet resistances even lower than those predicted by eq 5 may be attained.

CONCLUSIONS

In summary, we have found that nanostructured thin films with transparency, $T \sim 90\%$, tend to fall in the percolative regime. This means the DC conductivity is lower than in the bulk regime, resulting in higher than expected sheet resistances, R_s. We have developed a simple model which relates T to R_s in this percolative regime. This is controlled by a percolative figure of merit, Π. High values of Π, leading to high T and low R_s, are found when $\sigma_{DC,B}$ is high but σ_{Op} is low. In addition, the percolative exponent must be low, as must the film thickness at which the conductivity becomes thickness-dependent (t_{min}). This model fits well to data for networks of carbon nanotubes, metallic nanowires, graphene, and silver platelets. We show that t_{min} scales linearly with the smallest dimension of the nanostructure making the film. This shows that low diameter nanowires/nanotubes or thin platelets are best for transparent conducting applications. We show that networks of AgNWs with $D = 20$ nm should display $R_s = 10$ $\Omega/\square$ for $T = 90\%$.

METHODS

Preparation of Films of Silver Flakes. Silver flakes were purchased from Ferro (silver flake SF 77A), while isopropyl alcohol (IPA) was purchased from Aldrich. The silver flakes were heated to 160 °C for 0.5 h in an oven prior to suspension in IPA. The silver flakes were then added to IPA such that the silver concentration was 0.5 mg/mL. This dispersion was then sonicated for 2 h in a sonic bath (Branson 1510 MT). The resulting dispersions were vacuum-filtered using porous cellulose filter membranes (MF-Millipore membrane mixed cellulose esters, hydrophilic, 0.025 μm, 47 mm) to give thin films. The thickness of these films was controlled by the volume of dispersion filtered and hence the mass deposited. The films were then transferred to polyethylene terephthalate (PET) using IPA to adhere the film to the substrate. The cellulose filter membrane was removed using acetone vapor followed by immersion in acetone baths.

Optical transmission spectra were recorded in the visible range (400−800 nm) using a Varian Cary 6000i. In all cases, PET was used as the reference. Sheet resistance measurements were made using the four-probe technique with silver electrodes of dimensions and spacings typically of approximately millimeter size and a Keithley 2400 source meter. Flake and film thicknesses were gauged by measuring the height profile of a fractured cross section for a number of films of various thickness. This was achieved by mounting the sample parallel to electron beam in a Zeiss Ultra plus SEM. Electrical properties of the flake networks are given in the Supporting Information.

Supporting Information Available: Properties of Ag flake networks. Variation of σ_{DC} with D for metallic nanowire networks. Supporting figures. This material is available free of charge *via* the Internet at http://pubs.acs.org.

REFERENCES AND NOTES

1. Chen, Z.; Cotterell, B.; Wang, W. The Fracture of Brittle Thin Films on Compliant Substrates in Flexible Displays. *Eng. Fract. Mech.* **2002**, *69*, 597–603.
2. Leterrier, Y.; Medico, L.; Demarco, F.; Manson, J. A. E.; Betz, U.; Escola, M. F.; Olsson, M. K.; Atamny, F. Mechanical Integrity of Transparent Conductive Oxide Films for Flexible Polymer-Based Displays. *Thin Solid Films* **2004**, *460*, 156–166.
3. De, S.; Coleman, J. N. Are There Fundamental Limitations on the Sheet Resistance and Transmittance of Thin Graphene Films? *ACS Nano* **2010**, *4*, 2713–2720.
4. Dan, B.; Irvin, G. C.; Pasquali, M. Continuous and Scalable Fabrication of Transparent Conducting Carbon Nanotube Films. *ACS Nano* **2009**, *3*, 835–843.
5. De, S.; Lyons, P. E.; Sorrel, S.; Doherty, E. M.; King, P. J.; Blau, W. J.; Nirmalraj, P. N.; Boland, J. J.; Scardaci, V.; Joimel, J.; *et al.* Transparent, Flexible, and Highly Conductive Thin Films Based on Polymer-Nanotube Composites. *ACS Nano* **2009**, *3*, 714–720.
6. Doherty, E. M.; De, S.; Lyons, P. E.; Shmeliov, A.; Nirmalraj, P. N.; Scardaci, V.; Joimel, J.; Blau, W. J.; Boland, J. J.; Coleman, J. N. The Spatial Uniformity and Electromechanical Stability of Transparent, Conductive Films of Single Walled Nanotubes. *Carbon* **2009**, *47*, 2466–2473.
7. Geng, H. Z.; Kim, K. K.; So, K. P.; Lee, Y. S.; Chang, Y.; Lee, Y. H. Effect of Acid Treatment on Carbon Nanotube-Based Flexible Transparent Conducting Films. *J. Am. Chem. Soc.* **2007**, *129*, 7758–7759.
8. Hu, L.; Hecht, D. S.; Gruner, G. Percolation in Transparent and Conducting Carbon Nanotube Networks. *Nano Lett.* **2004**, *4*, 2513–2517.
9. Wu, Z. C.; Chen, Z. H.; Du, X.; Logan, J. M.; Sippel, J.; Nikolou, M.; Kamaras, K.; Reynolds, J. R.; Tanner, D. B.; Hebard, A. F.; *et al.* Transparent, Conductive Carbon Nanotube Films. *Science* **2004**, *305*, 1273–1276.
10. Chandra, B.; Afzali, A.; Khare, N.; El-Ashry, M. M.; Tulevski, G. S. Stable Charge-Transfer Doping of Transparent Single-Walled Carbon Nanotube Films. *Chem. Mater.* **2010**, *22*, 5179–5183.
11. Green, A. A.; Hersam, M. C. Solution Phase Production of Graphene with Controlled Thickness *via* Density Differentiation. *Nano Lett.* **2009**, *9*, 4031–4036.
12. Li, Z. R.; Kandel, H. R.; Dervishi, E.; Saini, V.; Xu, Y.; Biris, A. R.; Lupu, D.; Salamo, G. J.; Biris, A. S. Comparative Study on Different Carbon Nanotube Materials in Terms of Transparent Conductive Coatings. *Langmuir* **2008**, *24*, 2655–2662.
13. Manivannan, S.; Ryu, J. H.; Jang, J.; Park, K. C. Fabrication and Effect of Post Treatment on Flexible Single-Walled Carbon Nanotube Films. *J. Mater. Sci.* **2010**, *21*, 595–602.
14. Pei, S. F.; Du, J. H.; Zeng, Y.; Liu, C.; Cheng, H. M. The Fabrication of a Carbon Nanotube Transparent Conductive Film by Electrophoretic Deposition and Hot-Pressing Transfer. *Nanotechnology* **2009**, *20*, 235707.
15. Fanchini, G.; Miller, S.; Parekh, L. B.; Chhowalla, M. Optical Anisotropy in Single-Walled Carbon Nanotube Thin Films: Implications for Transparent and

Conducting Electrodes in Organic Photovoltaics. *Nano Lett.* **2008**, *8*, 2176–2179.

16. Parekh, B. B.; Fanchini, G.; Eda, G.; Chhowalla, M. Improved Conductivity of Transparent Single-Wall Carbon Nanotube Thin Films *via* Stable Postdeposition Functionalization. *Appl. Phys. Lett.* **2007**, *90*, 121913.

17. Unalan, H. E.; Fanchini, G.; Kanwal, A.; Du Pasquier, A.; Chhowalla, M. Design Criteria for Transparent Single-Wall Carbon Nanotube Thin-Film Transistors. *Nano Lett.* **2006**, *6*, 677–682.

18. De, S.; Higgins, T.; Lyons, P. E.; Doherty, E. M.; Nirmalraj, P. N.; Blau, W. J.; Boland, J. J.; Coleman, J. N. Silver Nanowire Networks as Flexible, Transparent, Conducting Films: Extremely High DC to Optical Conductivity Ratios. *ACS Nano* **2009**, *3*, 1767–1774.

19. Lee, J. Y.; Connor, S. T.; Cui, Y.; Peumans, P. Solution-Processed Metal Nanowire Mesh Transparent Electrodes. *Nano Lett.* **2008**, *8*, 689–692.

20. Rathmell, A. R.; Bergin, S. M.; Hua, Y. L.; Li, Z. Y.; Wiley, B. J. The Growth Mechanism of Copper Nanowires and Their Properties in Flexible, Transparent Conducting Films. *Adv. Mater.* **2010**, *22*, 3558–3563.

21. Wu, H.; Hu, L.; Rowell, M. W.; Kong, D.; Cha, J. J.; McDonough, J. R.; Zhu, J.; Yang, Y.; McGehee, M. D.; Cui, Y. Electrospun Metal Nanofiber Webs as High-Performance Transparent Electrode. *Nano Lett.* **2010**, *10*, 4242–4248.

22. Wu, J. B.; Agrawal, M.; Becerril, H. A.; Bao, Z. N.; Liu, Z. F.; Chen, Y. S.; Peumans, P. Organic Light-Emitting Diodes on Solution-Processed Graphene Transparent Electrodes. *ACS Nano* **2010**, *4*, 43–48.

23. Blake, P.; Brimicombe, P. D.; Nair, R. R.; Booth, T. J.; Jiang, D.; Schedin, F.; Ponomarenko, L. A.; Morozov, S. V.; Gleeson, H. F.; Hill, E. W.; *et al.* Graphene-Based Liquid Crystal Device. *Nano Lett.* **2008**, *8*, 1704–1708.

24. De, S.; King, P. J.; Lotya, M.; O'Neill, A.; Doherty, E. M.; Hernandez, Y.; Duesberg, G. S.; Coleman, J. N. Flexible, Transparent, Conducting Films of Randomly Stacked Graphene from Surfactant-Stabilized, Oxide-Free Graphene Dispersions. *Small* **2009**, *6*, 458.

25. Eda, G.; Fanchini, G.; Chhowalla, M. Large-Area Ultrathin Films of Reduced Graphene Oxide as a Transparent and Flexible Electronic Material. *Nat. Nanotechnol.* **2008**, *3*, 270–274.

26. Fraser, D. B.; Cook, H. D. Highly Conductive, Transparent Films of Sputtered In2-Xsnxo3-Y. *J. Electrochem. Soc.* **1972**, *119*, 1368.

27. Ghosh, D. S.; Chen, T. L.; Pruneri, V. High Figure-of-Merit Ultrathin Metal Transparent Electrodes Incorporating a Conductive Grid. *Appl. Phys. Lett.* **2010**, *96*, 041109.

28. Gordon, R. G. Criteria for Choosing Transparent Conductors. *MRS Bull.* **2000**, *25*, 52.

29. Haacke, G. New Figure of Merit for Transparent Conductors. *J. Appl. Phys.* **1976**, *47*, 4086–4089.

30. Jain, V. K.; Kulshreshtha, A. P. Indium-Tin-Oxide Transparent Conducting Coatings on Silicon Solar-Cells and Their Figure of Merit. *Sol. Energy Mater.* **1981**, *4*, 151–158.

31. Shim, B. S.; Zhu, J. A.; Jan, E.; Critchley, K.; Kotov, N. A. Transparent Conductors from Layer-by-Layer Assembled Swnt Films: Importance of Mechanical Properties and a New Figure of Merit. *ACS Nano* **2010**, *4*, 3725–3734.

32. Dressel, M.; Gruner, G. *Electrodynamics of Solids: Optical Properties of Electrons in Matter*; Cambridge University Press: Cambridge, UK, 2002.

33. Scardaci, V.; Coull, R.; Coleman, J. N. Very Thin Transparent, Conductive Carbon Nanotube Films on Flexible Substrates. *Appl. Phys. Lett.* **2010**, *97*, 023114.

34. Stauffer, D. S.; Aharony, A. *Introduction to Percolation Theory*; Taylor & Francis: London, 1994.

35. Blighe, F. M.; Hernandez, Y. R.; Blau, W. J.; Coleman, J. N. Observation of Percolation-like Scaling—Far from the Percolation Threshold—in High Volume Fraction, High Conductivity Polymer−Nanotube Composite Films. *Adv. Mater.* **2007**, *19*, 4443.

36. Dunbar, A. D. F.; Partridge, J. G.; Schulze, M.; Brown, S. A. Morphological Differences between Bi, Ag and Sb Nano-Particles and How They Affect the Percolation of Current through Nano-Particle Networks. *Eur. Phys. J. D* **2006**, *39*, 415–422.

37. Johner, N.; Grimaldi, C.; Balberg, I.; Ryser, P. Transport Exponent in a Three-Dimensional Continuum Tunneling-Percolation Model. *Phys. Rev. B* **2008**, *77*.

38. Zhang, Q. H.; Vichchulada, P.; Cauble, M. A.; Lay, M. D. Percolation in Networks of Aligned SWNTs Formed with Laminar Flow Deposition. *J. Mater. Sci.* **2009**, *44*, 1206–1211.

39. O'Connor, B.; Haughn, C.; An, K. H.; Pipe, K. P.; Shtein, M. Transparent and Conductive Electrodes Based on Unpatterned, Thin Metal Films. *Appl. Phys. Lett.* **2008**, *93*, 223304.

40. Nan, C.-W. *Prog. Mater. Sci.* **1993**, *37*, 1.

41. Bauhofer, W.; Kovacs, J. Z. A Review and Analysis of Electrical Percolation in Carbon Nanotube Polymer Composites. *Compos. Sci. Technol.* **2009**, *69*, 1486–1498.

42. Balberg, I. Tunnelling and Nonuniversal Conductivity in Composite-Materials. *Phys. Rev. Lett.* **1987**, *59*, 1305–1308.

43. Balberg, I. Limits on the Continuum-Percolation Transport Exponents. *Phys. Rev. B* **1998**, *57*, 13351–13354.

44. Kogut, P. M.; Straley, J. P. Distribution-Induced Non-universality of the Percolation Conductivity Exponents. *J. Phys. C* **1979**, *12*, 2151–2159.

45. Grimaldi, C.; Balberg, I. Tunneling and Nonuniversality in Continuum Percolation Systems. *Phys. Rev. Lett.* **2006**, *96*.

46. Nirmalraj, P. N.; Lyons, P. E.; De, S.; Coleman, J. N.; Boland, J. J. Electrical Connectivity in Single-Walled Carbon Nanotube Networks. *Nano Lett.* **2009**, *9*, 3890–3895.

47. Bid, A.; Bora, A.; Raychaudhuri, A. K. Temperature Dependence of the Resistance of Metallic Nanowires of Diameter ≥15 nm: Applicability of Bloch-Gruneisen Theorem. *Phys. Rev. B* **2006**, *74*.

48. Wiley, B. J.; Wang, Z. H.; Wei, J.; Yin, Y. D.; Cobden, D. H.; Xia, Y. N. Synthesis and Electrical Characterization of Silver Nanobeams. *Nano Lett.* **2006**, *6*, 2273–2278.

49. Hecht, D.; Hu, L. B.; Gruner, G. Conductivity Scaling with Bundle Length and Diameter in Single Walled Carbon Nanotube Networks. *Appl. Phys. Lett.* **2006**, *89*.

50. Lyons, P. E.; De, S.; Blighe, F.; Nicolosi, V.; Pereira, L. F. C.; Ferreira, M. S.; Coleman, J. N. The Relationship between Network Morphology and Conductivity in Nanotube Films. *J. Appl. Phys.* **2008**, *104*, 044302.